Kinetics of Mixed-Bed Deionization: I

NORMAN W. FRISCH and ROBERT KUNIN

Rohm & Haas Company, Philadelphia, Pennsylvania

Mixed-bed deionization of 0.0002 to 0.01N sodium chloride solutions at flow rates in the range of 3 to 70 gal./(min.) (sq. ft.) with bed depths of 0.25 to 3.2 ft. was investigated. The rate of ion exchange was found to be limited by a liquid-film mass transfer mechanism in the high purity water range (< 1 μ micromho/cm. effluent conductivity).

The magnitude of the temperature effect in the range 15° to 45°C. is given. Methods for prediction of effect of both changes in particle size distribution and incomplete regeneration of the component ion exchange resins are presented. A tentative correlation is given which estimates the effect of solute and solvent species.

Mixed-bed deionization, first devised by Kunin (*7*), serves as an economical and convenient means for the production of high purity water. In particular mixed-bed water of extraordinary quality is routinely produced for boiler feed water, nuclear reactor water, for the electronic and chemical industries, and for a variety of other large-scale applications. Small space requirement, uniform quality of effluent in intermittent service, and maintenance of a neutral effluent are important additional advantages of this technique. In addition to water many aqueous as well as nonaqueous solutions are rendered free of electrolyte in a simple operation.

Present day use of mixed-bed deionization for the above applications and in particular for the treatment of low level solids water (condensate) requires realistic estimates of mixed-bed performance. The use of mixed-bed units on an emergency standby basis on naval vessels, on which floor space is at a premium, indicates that a complete definition of the performance of these units must be secured. A review of the literature on this subject reveals several general investigations (*9, 10, 11*) but only one systematic study (*1*) of the variables involved in determining leakage-capacity relationship.

The latter work of Caddell and Moison (*1*) presented breakthrough curves for a mixed-bed unit of fixed bed depth operated over 5 to 100 gal./(min.)(sq. ft.) flow rates and containing from 3 to 192 p.p.m. of salt (principally aluminum) content. Unfortunately these results were not correlated in a rational fashion which might shed light on the mechanism of exchange or evolve a design expression. Furthermore the use of this salt system (aluminum nitrate with traces of the nitrate salts of magnesium, ferric, nickel, and chromium) presents the possibility of colloidal leakage. The high level of nitrate ion presents the possibility of incomplete regeneration of the anion resin, or at least nonreproducible regeneration in view of the variable nature of the loading cycle parameters. Despite this limitation this work is of value in pointing out the general applicability of mixed-bed deionization over a wide range of flow rates and concentrations.

The present study was undertaken to gain an improved understanding of the kinetics of this ion exchange operation. In particular, knowledge of the effect on performance of influent concentration, flow rate, bed depth, and temperature was desired. A need for a rational expression for the effect of particle size on mixed-bed performance was also evident.

EXPERIMENTAL APPARATUS AND PROCEDURE

Figure 1 is a diagram of the experimental equipment. It is composed of five sections: a solution storage section, flow control and measurement devices, the deionization unit, temperature control equipment, and conductivity measurement and recording devices.

The storage section, composed of polyethylene carboys, has a capacity of 525 liter. The carboys were charged by filling with mixed-bed effluent (specific conductivity <0.06 micromho/cm.) after addition of the calculated quantity of analytical reagent grade sodium chloride to the carboys. Each carboy was protected from atmospheric contamination by use of ascarite-containing guard tubes. Mixing of carboy solution was effected by circulation of the solution through the storage units. Complete homogenization was checked initially by conductivity measurement and verified by titration.

Flow was controlled by use of a U pump equipped with Kel-F body and alumina ceramic ball checks and piston. Two pumps with different piston diameters and stroking speeds were used interchangeably and could cover the range of 2 to >100 (gal.)/(min.)(sq. ft.). Each unit was fitted with an airdome which eased out pulsations. In order to maintain constancy of flow over long periods of time it was found necessary to control the suction level to the pump and also to use a back-pressure valve on the pump discharge side to overshadow any variations in pressure drop through the resin bed. The suction-level control utilized a polyethylene float and microswitch arrangement which actuated an air-operated diaphragm valve which controlled the flow of feed to the lower carboys through rubber tubing. The back-pressure valve was constructed of Kel-F and utilized a spring loaded Teflon diaphragm. Inter-

Norman W. Frisch is with Princeton Chemical Research, Incorporated, Princeton, New Jersey.

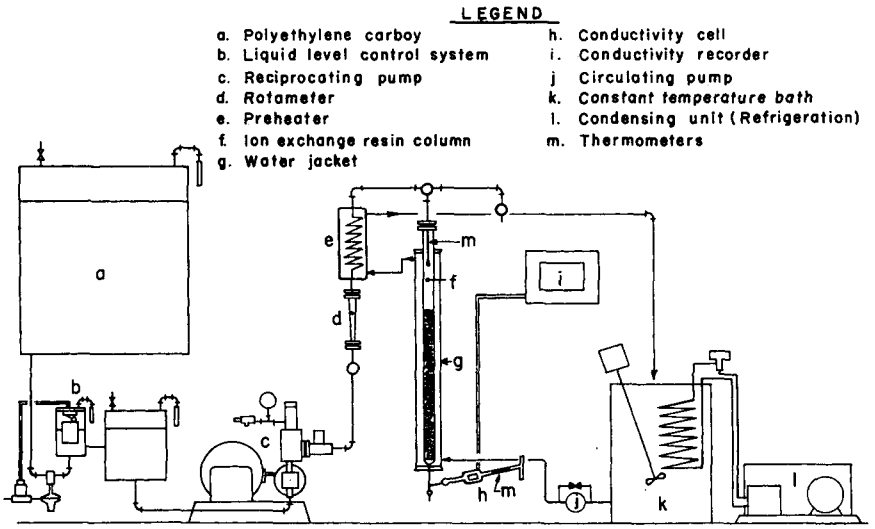

Fig. 1. Schematic arrangement of experimental equipment.

changeable rotameters with Pyrex or sapphire floats permitted approximate setting of flow rate. Flow rate was periodically accurately measured by checking the effluent volume collected in a timed period. The flow rate was sufficiently accurate ($<1\%$) that the effluent volume could be calculated on the basis of elapsed time and measured flow rate.

The deionization unit consisted of a ½-in. I.D. Pyrex glass pipe column, 48 in. long. A fritted glass disk of coarse porosity was sealed into the bottom of the column and served as a resin support. Feed lines to the unit from the pump were constructed of ¼-in. Pyrex glass pipe with appropriate pressure stop cocks and fittings. Gaskets were of Teflon. A water jacket enclosed the deionization unit, and a preheater unit consisting of glass coil and jacket served to bring feed solution to appropriate temperature.

A constant temperature bath was modified by addition of a condensing unit. Close temperature control was obtained over a wide temperature range (5° to 60°C). Water from the bath was pumped to the water jacket surrounding the deionization column and thence to the preheater jacket, and returned to the bath. Temperature control in the jacket was maintained within ± 0.2°C. of desired temperature.

Column effluent was monitored with a glass conductivity flow cell. The cell constant was periodically checked against standard potassium chloride solution. Conductivity readings were recorded on a recorder designed to permit accurate readings over a wide conductivity range.

Concentration of salt solutions was determined by titration against standard 0.02N silver nitrate with dichlorofluorescin used as an adsorption indicator. Titrations were performed in solutions 0.005N sodium chloride or higher in concentration. More dilute solutions were concentrated by evaporation in the presence of a nitrogen stream. The accuracy of this technique was found to be about 2 parts per thousand.

The resin used in the study was a standard production nuclear grade mixture of a strongly acidic cation exchange resin, and a strongly basic anion exchange resin. A weighed charge of resin was intermittently added to the ion exchange column containing a minimum quantity of water. After the bed was charged, it was homogenized by stirring with a rod. Water level was increased to 6 in. above top of bed. After temperature in the water jacket was brought to desired value, solution was pumped through preheater into column and exited through flow cell. Runs were continued in all cases until effluent conductivity increased to 1.0 micromho/cm. Each run was made with a fresh sample of mixed-bed ion exchange resin obtained from a standard production batch.

The conductance of the effluent solution was taken as the sum of the contributions of the salt and the solvent. The contribution of the salt content was calculated by use of the equivalent conductance values of Gunning and Gordon (3). The conductance of water at 25°C. was taken as 0.055 micromho/cm. A conductivity endpoint (at 25°C.) of 1.0 micromho/cm. was convenient and of practical significance for calculation of fractional leakage and utilization values necessary for the kinetic calculations.

As noted it was convenient to weigh out sample charges of ion exchange resin for each run. Since the properties of the individual cation and anion exchange resins are generally referred to their standard ionic forms, Na^+ and Cl^- respectively, it is desirable to refer a weighed charge to a volume basis of the exhausted form under standard conditions (backwashed and drained). Capacity measurements were performed on samples of the resin mixture and used in the calculation of utilization values. For the purpose of surface-area estimation, a weighed charge of resin was screened and the total surface area of each resin was calculated from the particle size distribution. Void fraction was calculated on the basis of the packing of the resin and the true density of the mixed-bed resin.

THEORY

Mixed-bed deionization is conceived as the simultaneous exchange of cations and anions by an intimate mixture of cation and anion exchange resins in the hydrogen- and hydroxyl-ion forms respectively. The concept of simultaneous exchange arises from the vast difference in exchange rates noted with a salt as compared with a nonneutral species (acid or base) in contact with a completely dissociated anion or cation exchange resin respectively. This distinction in behavior is largely based on the differences in equilibria between the salt-splitting and the neutralization reaction. For this reason it is practical and convenient to conceive an equivalent exchange system consisting of a salt-removing resin, which releases in the process an equivalent quantity of water. In this system the solute, both in the liquid and resin phases, would be the salt itself, rather than the individual ions. Based on this model system a kinetic theory of mixed-bed deionization is evolved.

Consider a fixed-bed deionization unit of constant cross-sectional area. Equivalent quantities of regenerated resins of the strongly dissociated (anion and cation) types, uniformly distributed throughout the column, are represented by particles of the salt-removing resin. No assumption of uniform resin particle size is made, although changes in particle size due to shrinkage during exhaustion are neglected. Initially the void liquid is pure solvent. Solution with a time-independent salt content is deionized by passage through the ion exchange resin bed at a constant flow rate. Uniform distribution of solution over the cross-sectional area is assumed. Isothermal operation is presumed.

The conservation equation for the solute for a differential bed thickness indicates that the quantity of a component removed from solution must equal the gain of that component in the ion exchange resin and in the voids of the differential element. Longitudinal diffusion is neglected:

$$\left[\frac{\partial c}{\partial v}\right]_{V_F} + f_E\left[\frac{\partial c}{\partial V_F}\right]_v + \rho_b\left[\frac{\partial q}{\partial V_F}\right]_v = 0 \qquad (1)$$

It is convenient to make a change in variable to use $(V_F - vf_E)$, the downstream solution volume, instead of V_F:

$$\left[\frac{\partial c}{\partial v}\right]_{(V_F - vf_E)} + \rho_b\left[\frac{\partial q}{\partial (V_F - vf_E)}\right]_v = 0 \qquad (2)$$

The boundary conditions for this operation, expressed in terms of the solute, are

$$c = c_o \qquad V_F \geq 0 \qquad v = 0 \qquad (3a)$$

$$q = q_o \qquad V_F = 0 \qquad v \geq 0 \qquad (3b)$$

$$Q \geq q_o > 0 \qquad (3c)$$

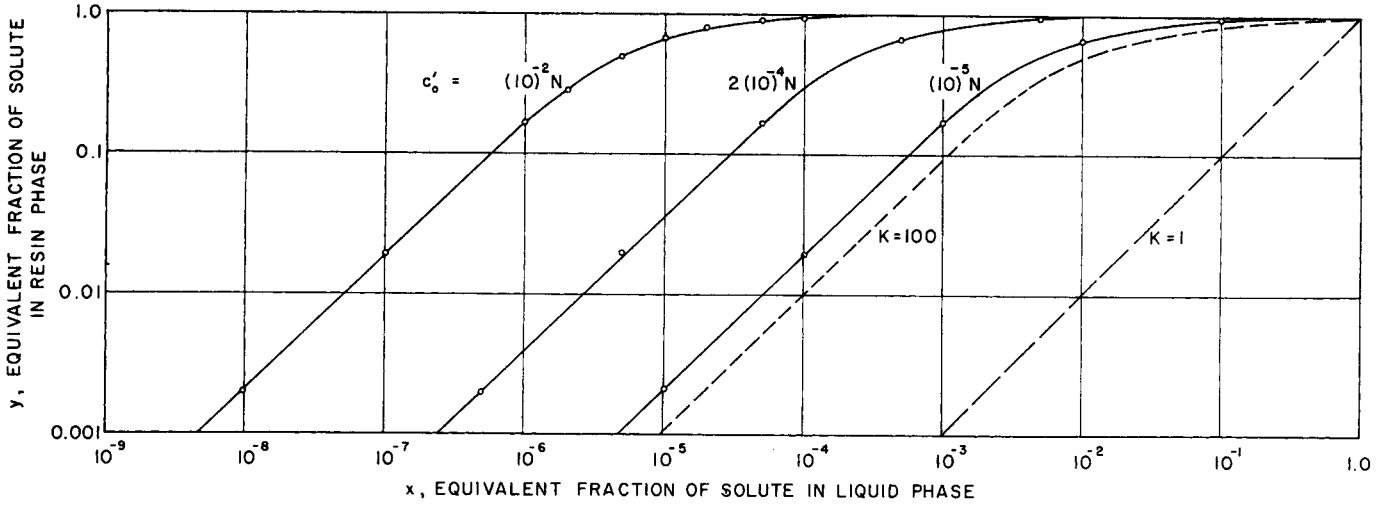

Fig. 2. Calculated mixed bed deionization equilibria.

In a mixed-bed deionization process, generally limited to feed concentrations on the order of 0.01-0.02 N, the concentration of solute is quickly reduced to extremely low values ($< 10^{-5}$ N). Under these conditions it seems likely that diffusion across the liquid film surrounding each resin particle would be the rate controlling process in the ion exchange operation. One assumes that mixed-bed operation in this concentration range with commercial resins of moderate cross linking is governed by a liquid-film mechanism. The rate equation expressing this mechanism is

$$\frac{dq}{dt} = k_f a(c - c^*) \qquad (4)$$

The equilibria which describes the mixed-bed deionization operation consists of three basic steps:

$$R_C H^+ + B^+ \rightleftharpoons R_C B^+ + H^+, K_I \qquad (5a)$$

$$R_A OH^- + A^- \rightleftharpoons R_A A^- + OH^-, K_{II} \qquad (5b)$$

$$H^+ + OH^- \rightleftharpoons H_2O, K_W \qquad (5c)$$

Calculation of an exact isotherm results from a knowledge of the three equilibrium constants and the principle of electrical neutrality. In general K_I and K_{II} are functions of the concentration of B and A in the individual resin phases. Rather than reporting the complex result of the complete calculation, one represents the solution for the equilibrium with K_I equal to K_{II} ($= K$) and taken independent of concentration by the following expression:

$$x^* = \frac{-\left[\frac{c'_o(1-x^*)}{y} - c'_o + \frac{\sqrt{K_W}}{K}\right] + \sqrt{\left[\frac{c'_o(1-x^*)}{y} - c'_o + \frac{\sqrt{K_W}}{K}\right]^2 + 4c'_o\frac{\sqrt{K_W}}{K}}}{2c'_o} \qquad (6)$$

The x^* value requires definition. Under ordinary circumstances it represents the equivalent fraction of a species in solution. In deionization studies the counterion is largely removed from participation in the ionic equilibrium by neutralization to form water. In this case the total ionic concentration of anion (or cation) is not constant. In this instance it is appropriate to define x^* as the ratio of the equilibrium concentration of the solute to its initial concentration value.

Equation (6) indicates the deionization equilibrium is strongly influenced by the feed concentration of salt. The isotherm represented by Equation (6) was calculated for 25°C. for c'_o values of $(10)^{-2}$, $2(10)^{-4}$, and $(10)^{-5}$ N (Figure 2). The latter concentration, equivalent to 0.5 p.p.m. (as calcium carbonate), is fairly typical of the lowest concentration commonly encountered as mixed-bed feed solution. It is apparent that although the isotherm is strongly concentration dependent, it is also strongly irreversible in all cases examined. Consequently the equilibrium is herein described:

$$c^* = 0 \qquad q < Q \qquad (7a)$$

$$c^* > 0 \qquad q = Q \qquad (7b)$$

The solution to Equations (2), (3), (4), and (7) for liquid-phase concentration has been given by Drew, Spooner, and Douglas and was reported

TABLE 1

Ion exchange resin characteristics

Amberlite XE-150

Batch #58-1918

$\rho_b = 52.5$ lb. moist regenerated resin / cu. ft. exhausted volume

$f_B = 0.445$

$Q = 8.96\,(10)^{-4}$ lb. equivalent / lb. most resin (regenerated resin)

Particle size distribution (regenerated resin)

	anion resin	cation resin
$\bar{d}_R$	0.0630 cm.	0.0760 cm.
σ_R	1.22	1.25
W_R	0.582	0.418

$\rho_R = 1.096$ g./ml. anion resin, 1.208 g./ml. cation resin

Specific surface area

$a_A = 25.4$ sq. ft. / lb. moist regenerated resin

$a_C = 13.7$ sq. ft. / lb. moist regenerated resin

by Klotz (6). It is based on the constant band-width concept which is more likely to apply as the degree of irreversibility of the exchange reaction increases:

$$\ln \frac{c}{c_o} = -\frac{k_f a \rho_b v}{L} \cdot \frac{c_o(V_F - v f_E)}{\rho_b v (Q - q_o)} < \frac{L}{k_f a \rho_b v} \qquad (8a)$$

and

$$\ln \frac{c}{c_o} = \frac{k_f a \rho_b v}{L} \left[\frac{c_o(V_F - v f_E)}{\rho_b v (Q - q_o)} - 1 \right] - 1, \qquad (8b)$$

$$1 + \frac{L}{k_f a \rho_b v} > \frac{c_o(V_F - v f_E)}{\rho_b v (Q - q_o)} > \frac{L}{k_f a \rho_b v}$$

Equation (8a) defines the preliminary constant composition period until

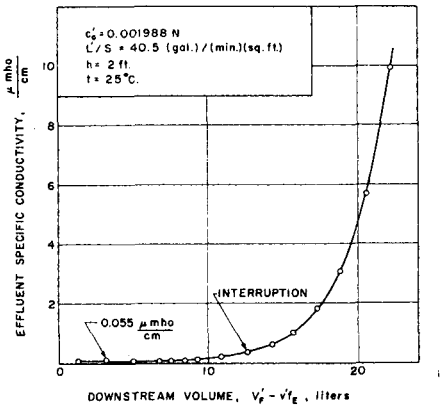

Fig. 3. Typical breakthrough curve (intermediate feed concentration).

the entrance face ($v = 0$) becomes saturated, $t = (Q - q_o)/(k_f a c_o)$. Equation (8b) predicts leakage values at all subsequent values of time, up to the time at which $c = c_o$. Complete lack of particle diffusional resistance is not necessary for Equations (8) to describe the breakthrough, since it can be readily shown, on the basis of a combined liquid-film and solid-shell particle rate equations, that in the low fractional endpoint leakage range involved in this study particle resistance influences only to a slight degree breakthrough characteristics.

If the value of c/c_o at the end point is small, say 0.05 or less, then the quantity $c_o(V_F - v f_E)/\rho_b v (Q - q_o)$ may be taken to denote the resin utilization of the regenerated ion exchange sites. A low level end point usually prevails in mixed-bed deionization operation, and consequently in subsequent development U will denote both this quantity and resin utilization. In operations involving higher values of c/c_o at the end point it is rather simple to correct the U term for the loss of resin loading due to ionic leakage. From (8b), for trace leakage end points

$$U = 1 + \frac{L}{k_f a \rho_b v} [1 + \ln c/c_o] \qquad (9)$$

The significance of the grouping of variables in equation (9) may be interpreted in various manners. The authors prefer to note that the loss in utilization due to the kinetic factor is proportional to the quantity $L/a\rho_b v$, the flow rate per unit surface area, and inversely proportional to the rate constant k_f. While the term $a\rho_b v$ depends upon resin properties and total resin charge, and L depends upon operating requirements, the mass transfer coefficient k_f depends upon resin properties, solution properties, bed geometry, and operating requirements.

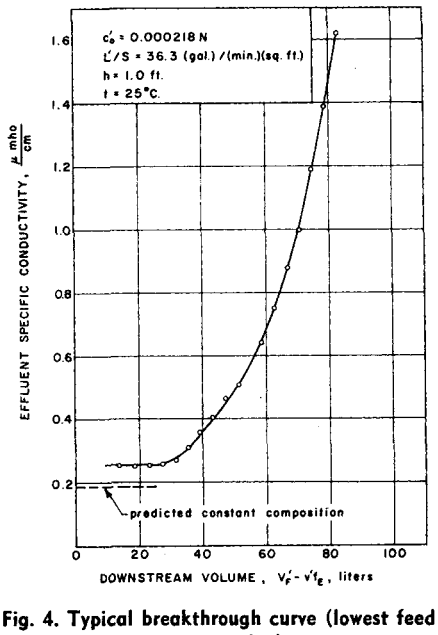

Fig. 4. Typical breakthrough curve (lowest feed concentration).

The formulation of an expression relating k_f to the pertinent variables is often approached from a dimensional analysis viewpoint, especially when complex geometrical flow patterns are involved. A suitable expression appears to be of the form

$$\frac{k_f d_p}{D} = \alpha (N_{Re}{}^m)(N_{Sc}{}^n) \qquad (10)$$

Inasmuch as solvents of varying viscosity and solutes of different diffusivities were not used in the column study, it is not possible to completely define the constants in Equation (10), although a fair estimate may be made of their magnitude.

The value of the pertinent a term in the combined constant $k_f a$ depends upon the particle size distribution of the ion exchange resin which possesses the smaller surface area (per unit mass of mixed-bed resin). The value of a is readily calculated for a log normal distribution of particle size for the controlling resin. The latter distribution is selected on the basis of both empirical and theoretical significance (5):

$$a_R = W_R \frac{6}{\rho_R} \sum \frac{\Delta W}{d_R} \qquad (11)$$

and

$$a_R = W_R \frac{6}{\rho_R} \frac{1}{\sqrt{2\pi} \log \sigma_R} \int_{-\infty}^{\infty} \frac{e^{\left\{ \frac{-\log^2 \frac{d_R}{\bar{d}_R}}{2 \log^2 \sigma_R} \right\}}}{d_R} d(\log d_R) \qquad (12)$$

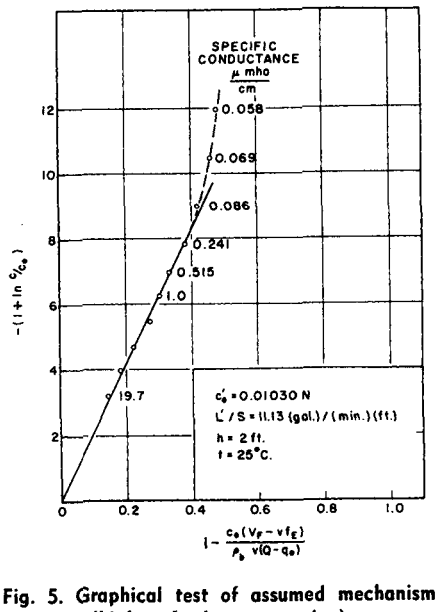

Fig. 5. Graphical test of assumed mechanism (highest feed concentration).

The value of the definite integral in (12) was evaluated with the resulting value:

$$a_R = W_R \frac{6\, e^{\frac{\log^2 \sigma_R}{2}}}{\rho_R \bar{d}_R} \qquad (13)$$

that is $\bar{d}_R\ e^{(-\log^2 \sigma_R)/(2)}$ is the effective particle size of a single resin which possesses a log normal distribution. For most commercial resins the value of $e^{(-\log^2 \sigma_R)/(2)}$ may be shown to be within 10% of unity. Thus the geometrical mean particle size defines the surface area of the resin.

CORRELATION OF EXPERIMENTAL RESULTS

Table 1 summarizes the pertinent properties.

Typical experimental breakthrough curves are shown in Figures 3 and 4, expressed in terms of experimentally meas-

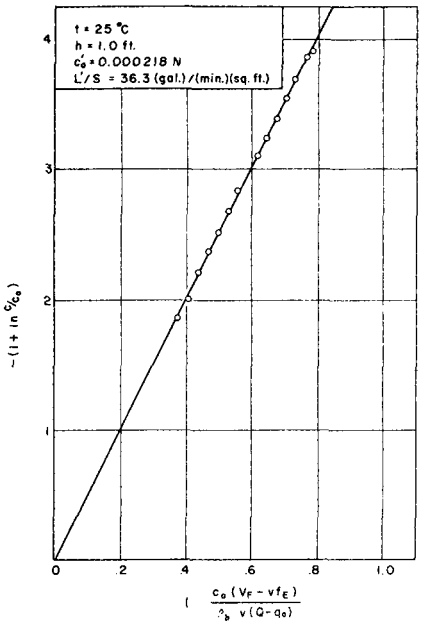

Fig. 6. Graphical test of assumed mechanism (lowest feed concentration).

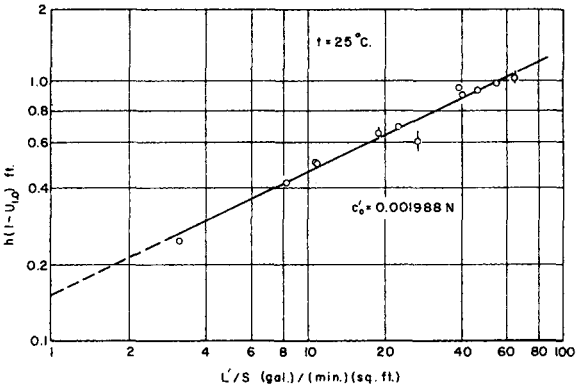

Fig. 8. Dependence of $h(1\text{-}U_{1.0})$ on mass flow rate (intermediate feed concentration).

ured quantities, specific conductance, and downstream volume. In many of the runs the constant composition phase of the cycles, predicted by Equation (8*a*), occurred with an effluent essentially free of salt (Figures 3). With excessively high mass flow rates, shallow beds, and high influent concentrations a constant finite leakage was detected (Figure 4). This is in agreement with Equation (8*a*).

While these figures present the appearance of typical ion exchange leakage curves, distinguishing features should be noted. The magnitude of the leakage is generally extraordinarily small compared with usual values experienced in ion exchange operations. Furthermore the breakthrough is quite sharp, in spite of the high flow rates and shallow beds examined in the investigation. Note that the maximum fractional leakage values represented in Figures 3 and 4 are only about 0.02 and 0.05 respectively. It is apparent that the kinetics of deionization are quite favorable.

The kinetic interpretation of the leakage curves can, ideally, be based on either Equation (8*a*) or (8*b*). Clearly the use of (8*b*) is preferable on two bases. Firstly the basis for evaluating the rate constant, if Equation (8*a*) is selected, depends upon measurement of either the leakage value c/c_o in the constant composition range or upon the duration of this phase of the cycle. The former cannot be measured with sufficient accuracy because of the low absolute value of the leakage and the attendant possibility of contamination. The latter value is poorly defined experimentally because of the curvature of the breakthrough curve at the beginning of the ascending leakage period. A practical reason for the selection of the latter phase of the leakage curve for the basis of the interpretation is that it actually defines the performance range of interest in most industrial installations. (Only in occasional laboratory studies would one be interested in preparing completely deionized water, corresponding to the constant composition period.)

The basis of interpretation Equation (8*b*) also presents an approach in which more than one or two measurements may serve to define the pertinent rate constants. By rearrangement of Equation (9) it is noted that the quantity $-(1 + \ln c/c_o)$ is proportion to $1 - c_o(V_F - vf_E)/\rho_b v(Q - q_o)$. Figures 5 and 6 are plots resulting from this test of the assumed mechanism. Linearity for these plots is good, although some curvature is noted as the effluent concentration range below 10^{-6}N (0.2 micromho/cm.) is examined. This minor deficiency is of little significance owing to the extreme ease of contamination in this low leakage range. More important is the good proportionality noted in the range of practical end points (1 to 0.2 micromho/cm.). For simplicity and practicality Table 2, which summarizes the performance at 25°C. at the highest concentration level, tabulates the value of $c_o(V - vf_E)/\rho_b(Q - q_o)$ that is U at a 1.0 micromho/cm. end point. These and the corresponding values at other concentrations are conveniently used for correlation purposes.

Rearrangement of Equation (9) to the form

$$h(1-U) = \frac{-(L/S)(1 + \ln c/c_o)}{k_f a \rho_b} \qquad (14)$$

and the usual assumption that k_f is primarily a function of mass flow rate in this system of fixed solute and solvent, operated at a constant temperature

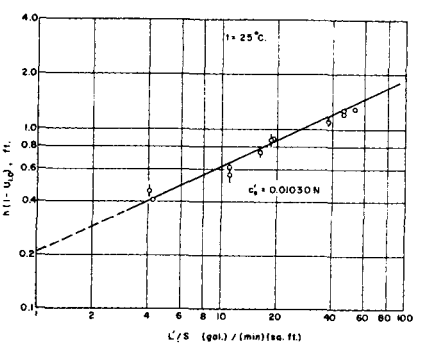

Fig. 7. Dependence of $h(1\text{-}U_{1.0})$ on mass flow rate (highest feed concentration).

Table 2. Typical Experimental Column Data

$c'_o = 0.01030$N, $t = 25$°C.

h, ft. Bed depth	L'/S, (gal.)/(min.)(sq. ft.) Flow rate	$U_{1.0}$, Utilization	$h(1\text{-}U_{1.0})$, ft.	
2.000	4.06	0.773	0.454	
0.500	4.26	0.181	0.409	
2.000	11.11	0.699	0.602	duplicate
2.000	11.13	0.693	0.614	duplicate
3.167	11.17	0.824	0.559	
3.167	16.24	0.764	0.746	
3.167	18.50	0.722	0.885	
2.000	19.05	0.555	0.890	
3.167	38.0	0.653	1.100	
3.167	46.0	0.617	1.212	
2.000	46.1	0.364	1.272	
3.167	53.8	0.589	1.300	

$$k_f = k_o\,(L/S)^m \qquad (15)$$

indicates a suitable graphical correlation technique is to plot log $h\ (1-U)$ vs. log L/S. Figures 7, 8, and 9 are plots of this nature for the 25°C. runs, each plot corresponding to a constant influent concentration c_o. The value of U and c correspond to the 1 micromho/cm. end point. Most of the data points are represented by circles with errors of ± 3% of $h\ (1-U)$; however several points, notably those pertaining to runs with high utilization values, are shown with the estimated larger errors. Rather well defined straight lines were drawn on each plot with a slope of $(1-m)$ of 0.48. This constancy of the exponent over a 25-fold range in flow rate is not unexpected. Values of $(k_o a\,\rho_b)$ ranged from 83.6 at the highest feed concentration down to 83.2 for the low salt-level runs. This constancy is a remarkable verification of the suitability of the assumed mechanism and model system.

Other support for the mechanism include the interrupted run depicted in Figure 3. With a particle diffusion mechanism a sharp decrease in effluent concentration would accompany start-up after an interruption. No such abrupt change in concentration is evident in either plot. The test of the assumed mechanism, based on Equation (8*a*), is shown on Figure 4. Both the predicted effluent concentration and downstream volume, which accumulates during the constant composition period, is shown by a dotted line. While the volume is in good agreement with the measured volume, there is a modest discrepancy in concentration value. The latter is not surprising in view of the absolute value of the salt leakage, about 1 $(10)^{-6}$N.

The derived value of the parameter $k_f a\,\rho_b$ is given by

$$k_f a\,\rho_b = 83.4\,(L/S)^{0.52} \qquad (16)$$

which when combined with Equation (9) results in an equation which defines the performance of the mixed-bed resin at 25°C.:

$$U_{1.0} = 1 + \frac{0.0332\,(L'/S)^{0.48}}{h}\,(1+\ln c/c_o) \qquad (17)$$

Several runs were made at 15° and 45°C., with a feed composition of $c_o' = 0.0103$N. Table 3 summarizes these data, while Figure 10 is the correlating plot. Values of $k_o a \rho_b$, at $c_o' = 0.01030$N, were 69.5 at 15°C., 83.4 at 25°C., and 128.7 at 45°C.

It is noted that $k_f a \rho_b/(L/S)^{0.52}$ depends upon the absolute temperature approximately as the 6.2 power, a value comparable to other findings in the field of diffusion through liquid films. In order to make an estimate of the exponent of the Schmidt group and the proportionality constant α in Equation (10) Figure 11 was prepared. Values of viscosity and density of the liquid phase were taken as that of pure water at the temperature under consideration, while diffusivity values are those for infinitely dilute sodium chloride solutions, as calculated from the Nernst equation. The temperature dependence of the limiting ionic mobilities necessary for the Nernst formulation was calculated from the data tabulated in the text of Harned and Owen (*4*).

In order to formulate the complete expression indicated by Equation (10) several points require clarification, namely the definitions of d_p, a, and Reynolds number. Effective particle diameter for both dimensionless groups was taken as the diameter of a particle whose surface area would be equal to the surface area of an equivalent mass of mixed-bed resin. Microscopic examination revealed that the surface roughness of the cation resin was appreciably greater than that of the anion resin; on this basis the value of a was taken as that of the anion resin (calculated value a_A = 25.4 sq. ft./lb. mixed-bed resin, a_C = 13.7 sq. ft./lb. mixed-bed resin). Reynolds number was defined in a manner which appears to be preferable for packed towers, namely

Table 3. Summary of Experimental Column Data

Effect of temperature

$c_o' = 0.0103$N, $t = 15$°C.

h, ft. Bed depth	L'/S, (gal.)/(min.)(sq. ft.) Flow rate	$U_{1.0}$, Utilization	$h\,(1\text{-}U_{1.0})$, ft.
0.833	5.80	0.308	0.577
1.000	6.91	0.364	0.638
2.000	9.12	0.620	0.760
3.166	11.4	0.764	0.750
2.000	20.2	0.524	0.950
3.166	53.3	0.415	1.850
	$t = 45$°C.		
0.500	5.98	0.283	0.358
3.166	10.1	0.892	0.342
0.833	12.8	0.449	0.459
1.000	20.3	0.381	0.618
2.000	37.9	0.630	0.740
2.000	52.1	0.557	0.875

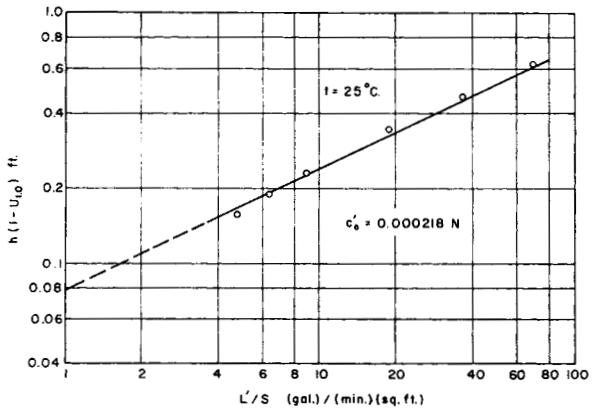

Fig. 9. Dependence of $h(1\text{-}U_{1.0})$ on mass flow rate (lowest feed concentration).

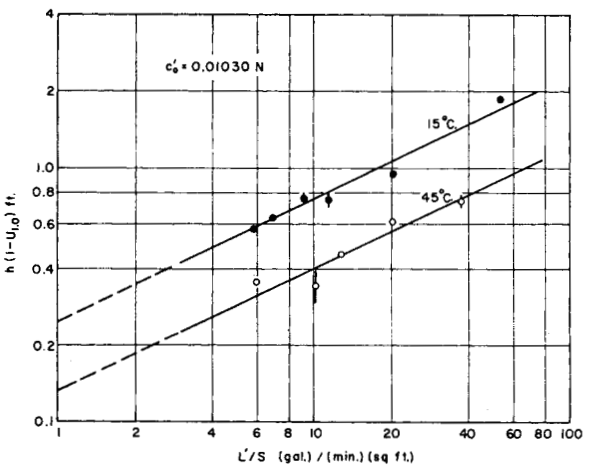

Fig. 10. Dependence of $h(1\text{-}U_{1.0})$ on mass flow rate at 15° and 45°C.

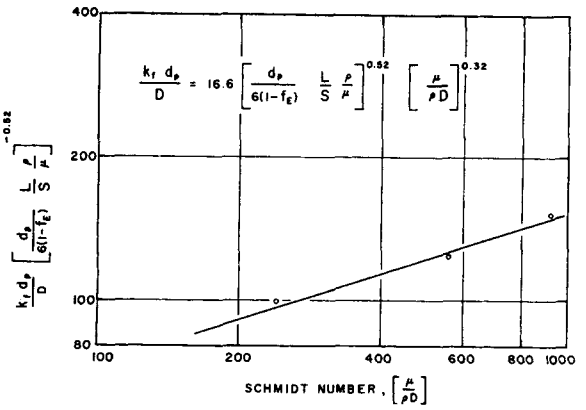

Fig. 11. Dependence of liquid-film coefficients on Schmidt group.

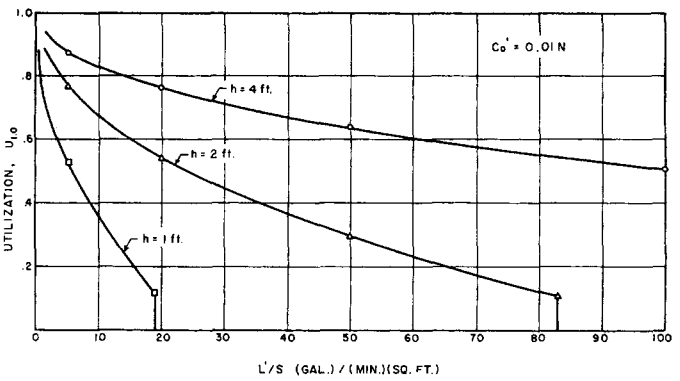

Fig. 12. Predicted performance of Amberlite XE-150 at 500 p.p.m. feed concentration.

$$R_s = \left[\frac{d_p f_B}{6(1-f_B)} \frac{L}{S f_B} \frac{\rho}{\mu}\right] \quad (18)$$

The tentative nature of this correlation must be realized; only a limited number of solute and solvents were investigated. Also the estimated nature of d_p is apparent. The equation which is derived from Figure 11 is

$$\frac{k_f d_p}{D} = 16.6\left[\frac{d_p}{6(1-f_B)} \frac{L}{S} \frac{\rho}{\mu}\right]^{0.52}\left[\frac{\mu}{\rho D}\right]^{0.32} \quad (19)$$

The form may be compared with the equation of Wilke and Hougen (*12*) derived from experiments involving transfer of water vapor from air flowing through beds of granular solids. In the authors' notation their expression is

$$\frac{k_f S f_B}{L} = 1.82\left[d_p \frac{L}{S} \frac{\rho}{\mu}\right]^{-0.51}\left[\frac{\mu}{\rho D}\right]^{-0.67} \quad (20)$$

By simple rearrangement and substitution for f_B, the following forms may be derived:

$$\frac{k_f d_p}{D} = 4.65\left[d_p \frac{L}{S} \frac{\rho}{\mu}\right]^{0.49}\left[\frac{\mu}{\rho D}\right]^{0.33} \quad \text{(Wilke)} \quad (21)$$

$$\frac{k_f d_p}{D} = 8.90\left[d_p \frac{L}{S} \frac{\rho}{\mu}\right]^{0.62}\left[\frac{\mu}{\rho D}\right]^{0.32} \quad \text{(Present work)} \quad (22)$$

While the forms are nearly equivalent, the discrepancy in coefficient warrants discussion. Two factors contribute to the higher coefficient noted in this study. Surface roughness of the ion exchange resin beads probably cause surface areas significantly higher than those calculated from the particle size distribution. Another important factor is that the diffusion constant in (19) is probably not best represented by that for sodium chloride but by the equimolal counter diffusion constant for chloride-hydroxide or sodium-hydrogen ion. This results in the liquid-film mass transfer coefficient being a function of composition; for the cation resin the form is $(k_f)_{Na}(k_f)_H/[(k_f)_{Na}x+(k_f)_H(1-x)]$. The diffusivity of acid or base is about half a magnitude higher than that of the neutral salt. These factors contribute to the increase in magnitude of the coefficient in Equation (19).

DESIGN CONSIDERATIONS

For the purpose of routine estimates of mixed-bed performance to a 1 micromho/cm. conductivity end point, plots similar to Figure 12 may be prepared based on Equation (17). In the case of the low concentration feed solutions Equation (17) is not applicable, since end point fractional leakage is quite appreciable. The calculation in this instance must be corrected for finite leakage during the run. Extrapolation to low concentrations can be performed with confidence as the liquid film transfer rate decreases with decreased concentration.

In some instances performance estimates may be required for resins of different particle size distributions than these examined in this study. Similarly the effect of different solutes may be required. The effect of particle size on a is calculated from Equation (13), while the effect of k_f is readily evaluated by Equation (19). The effect of solute diffusivity and solvent viscosity may also be predicted from Equation (19). Note that the influence of the latter variables on particle diffusivity may also require consideration. In particular, when several effects are required simultaneously, it may be convenient to take advantage of the simple form of Equation (8*b*) and of the known exponent in Equation (15). A single run under well-defined conditions will suffice for the determination of $(k_o a \rho_b)$. Generally utilization values of about 0.5 or less should be aimed for in this test for high accuracy in determining the unknown parameter.

Intermittent operation, common with some installations, presents little difficulty in design estimates. Capacity is unaltered in this situation owing to the nature of the controlling transfer mechanism.

In practice, regeneration is generally restricted to economic values, permitting treatment of a large quantity of solution per unit quantity of regenerant. The quantity (solution treated/regenerant consumed) is not maximized, since other (generally minor) costs must be considered. The practical regeneration level increases with decrease in influent concentration. In a particular case it is possible ideally to derive the same utilization fraction of the regenerated capacity regardless of the absolute value of the regenerated capacity. This is a consequence of the uniform distribution of the regenerated resin throughout the column owing to air mixing after the regeneration, and also a result of the nature of the controlling mechanism and equilibrium. With a liquid-film mechanism and an irreversible isotherm the unregenerated sites act as inert material, neither influencing the isotherm formulation nor the rate of transfer across the film. This approach is valid provided each resin particle in the bed is regenerated to finite degree during the regeneration operation. This limitation is necessary to preserve the constancy of the surface-area term in Equation (9). An estimate of the minimum regeneration level to achieve this limited degree of regeneration may be made by the equilibrium approach of Frisch (*2*); it is necessary to expend K_r equivalents per equivalent of each ion exchange resin in the operation.

In this study the authors operated with a small diameter column. This

was necessary so as not to exceed the limited salt solution storage capacity required in the case of dilute feed concentrations and also to make use of relatively small capacity noncontaminating pumps available commercially. In the range of normal voidage noted in ion exchange resin beds the fractional change in rate constant is only about one half that of the fractional change in void fraction causing this variation in rate constant. This is in agreement with the estimate of Leigh (8). With a ratio of average particle diameter to column diameter of about 18 the increase in f_B is small and probably contributes less than several percent difference in rate constant from that experienced in large diameter beds. No correction is warranted in this situation.

CONCLUSIONS

Mixed-bed deionization with conventional ion exchange resins proceeds with a liquid-film mechanism controlling the transfer rate. Performance in terms of effluent quality and throughput can be expressed in simple form. The effect of temperature was presented in terms of experimentally determined rate constants. The effect of particle size is predictable by the indicated equations. A correlation is given which predicts the effect of change in solute and solvent system. Fair agreement is noted between this tentative correlation and a previously published mass transfer expression.

ACKNOWLEDGMENT

The authors are grateful for the experimental assistance of S. C. Adams, D. G. Garaventi, and F. J. Zunino.

NOTATION

a = specific surface area of controlling resin based on mass of mixture, sq. ft./lb. moist mixed-bed resin

a_A, a_C, a_R = specific surface area of indicated resin based on mass of mixture, sq. ft./lb. moist mixed-bed resin

c = concentration of solute in liquid phase, lb. equivalents/cu. ft.

c_o = concentration of solute in feed solution to mixed bed, lb. equivalent/cu. ft.

c_o' = value of c_o expressed in normality, g. equivalent/liter

c^* = value of liquid-phase concentration which would be in equilibrium with resin concentration, lb. equivalents/cu. ft.

$\bar{d}_A, \bar{d}_C, \bar{d}_R$ = weight geometrical mean particle diameter of single resin species, ft.

d_p = effective diameter of mixed-bed resin, based on equivalent surface area, ft.

D = liquid-phase diffusivity of solute, sq. ft./min.

f_B = fractional void volume of bed, dimensionless

h = height of mixed-bed resin, based on exhausted form, ft.

k_f = liquid-film mass transfer coefficient, ft./min.

k_o = coefficient in Equation (15)

K = chemical equilibrium constant for exchange reaction, dimensionless

K_I = chemical equilibrium constant for exchange of solute salt with cation exchange resin, dimensionless

K_{II} = chemical equilibrium constant for exchange of solute salt with anion exchange resin, dimensionless

K_r = equilibrium constant for regeneration operation

K_W = ion product for water, $(\text{g. moles})^2/(\text{liter})^2$

L = flow rate, lb./min.

L' = flow rate, gal./min.

m = exponent in Equation (10), dimensionless

n = exponent in Equation (10), dimensionless

N_{Re} = Reynolds number, dimensionless

N_{Sc} = Schmidt number, dimensionless

q = concentration of solute in resin phase, lb. equivalents/lb. moist mixed-bed resin

q_o = concentration of solute in resin phase at time zero, lb. equivalents/lb. moist mixed-bed resin

Q = mixed-bed resin total capacity, lb. equivalents/lb. moist mixed-bed resin

R_A = anion exchange resin matrix

R_C = cation exchange resin matrix

S = cross-sectional area of mixed-bed unit, sq. ft.

t = time, min.

U = utilization of regenerated resin sites, dimensionless

$U_{1.0}$ = value of U at 1.0 micromho/cm. conductivity end point, dimensionless

v = bulk-packed volume of mixed bed, exhausted form, cu. ft.

v' = value of v, liters

V_F = volume of loading solution fed to column, cu. ft.

V'_F = value of V_F, liters

W_A, W_B, W_R = weight fraction of indicated resin species in mixed-bed resin, moist basis dimensionless

ΔW = weight fraction of single resin species within indicated particle size range, dimensionless

x = equivalent fraction of solute in solution phase, based on initial concentration, dimensionless

x^* = equilibrium equivalent fraction of solute in solution phase, based on initial concentration, which corresponds to y, dimensionless

y = equivalent fraction of solute in resin phase, dimensionless

Greek Letters

α = proportionality constant in Equation (10), dimensionless

μ = viscosity of liquid phase, lb./(ft.)(min.)

ρ = solution density, lb./cu. ft.

ρ_A, ρ_C, ρ_R = particle density of indicated resin species, lb. moist resin/cu. ft. particle volume

ρ_b = bulk density of mixed-bed resin, lb. moist mixed-bed resin/cu. ft. exhausted bulk volume

$\sigma_A, \sigma_B, \sigma_R$, = standard deviation of log normal distribution of a single resin particle size, dimensionless

Subscripts

A = anion exchange resin

C = cation exchange resin

R = either species of ion exchange resin

LITERATURE CITED

1. Caddell, J. R., and R. L. Moison, *Chem. Eng. Progr. Symposium Ser. No. 14*, **50**, 1 (1954).
2. Frisch, N. W., and F. X. McGarvey, *Chem. Eng. Progr. Symposium Ser. No. 24*, **55**, 51 (1959).
3. Gunning, H. E., and A. R. Gordon, *J. Chem. Phys.*, **10**, 126 (1942).
4. Harned, H. S., and B. B. Owen, "Physical Chemistry of Electrolytic Solutions," 2 ed., pp. 589-591, Reinhold, New York (1950).
5. Herdan, G., "Small Particle Statistics," pp. 112-113, Elsevier, Amsterdam, The Netherlands (1953).
6. Klotz, I. M., *Chem. Reviews*, **39**, 241 (1946).
7. Kunin, Robert, and F. X. McGarvey, *U.S.P. 2,578,937* (1951).
8. Leigh, T. F., Private communication.
9. McGarvey, F. X., and Robert Kunin, *Ind. Eng. Chem.*, **43**, 734 (1951).
10. Monet, G. P., *Chem. Eng. Progr.*, **52**, 299 (1956).
11. Thompson, Joseph, *et al.*, *Chem. Eng. Progr.*, **49**, 341, 437 (1953).
12. Wilke, C. R., and O. A. Hougen, *Trans. Am. Inst. Chem. Engrs.*, **41**, 445 (1945).

Manuscript received August 3, 1959; revision received February 11, 1960; paper accepted February 19, 1960.